Characterization of pK_a Values and Titration Shifts in the Cytotoxic Ribonuclease α-Sarcin by NMR. Relationship between Electrostatic Interactions, Structure, and Catalytic Function†

José Manuel Pérez-Cañadillas,‡ Ramón Campos-Olivas,‡,§ Javier Lacadena,|| Alvaro Martínez del Pozo,|| José G. Gavilanes,|| Jorge Santoro,‡ Manuel Rico,‡ and Marta Bruix*,‡

Instituto de Estructura de la Materia, Consejo Superior de Investigaciones Científicas, Serrano 119, 28006 Madrid, Spain, and Departamento de Bioquímica y Biología Molecular I, Facultad de Química, Universidad Complutense, 28040 Madrid, Spain

Received July 14, 1998; Revised Manuscript Received September 17, 1998

ABSTRACT: The electrostatic behavior of titrating groups in α-sarcin was investigated using ^{1}H NMR spectroscopy. A total of 209 chemical shift titration curves corresponding to different protons in the molecule were determined over the pH range of 3.0−8.5. Nonlinear least-squares fits of the data to simple relationships derived from the Henderson−Hasselbalch equation led to the unambiguous determination of pK_a values for all glutamic acid and histidine residues, as well as for the C-terminal carboxylate and most of the aspartic acids in the free enzyme. The ionization constants of catalytically relevant histidines, His50 and His137, and glutamic acid, Glu96, in the α-sarcin−2′-GMP complex were also determined. The pK_a values of 15 ionizable groups (C-carboxylate, six aspartic acids, four glutamic acids, and four histidines) were found to be close to their normal values. On the other hand, a number of side chain groups, including those in the active center, showed pK_a values far from their intrinsic values. Thus, the pK_a values for active site residues His50, Glu96, and His137 were 7.7, 5.2, and 5.8 in the free enzyme and 7.6, ∼4.8, and 6.8 in the α-sarcin−2′-GMP complex, respectively. The pK_a values and the activity profile against ApA, as a function of pH, are in agreement with the proposed enzymatic mechanism (in common with RNase T1 and the family of the microbial ribonucleases), in which Glu96 and His137 act as a general base and general acid, respectively. In almost all microbial ribonucleases, a Phe−His interaction is present, which affects the pK_a of one of the His residues at the active site (His137). The absence of this interaction in α-sarcin would explain the lower pK_a value of this His residue, and provides an explanation for the decreased RNase activity of this protein as compared to those of other microbial ribonucleases.

Electrostatic interactions are one of the forces known to contribute to the determination of the structure and dynamics of biological molecules. They play a prominent role in many aspects of protein biological function (*1*, *2*). Amino acids with ionizable side chains participate very often in enzyme catalytic reactions (*3*), as well as in ligand binding and molecular recognition processes involving proteins (*4*). Charge or dipolar interactions between amino acid side chains affect the stability of proteins, and they are, together with hydrogen bonds and hydrophobic interactions, the main energetic determinants of stability (*5*, *6*). The number of charged residues in a protein is usually low. However, changes in the ionization state for a few of these residues may drastically affect the stability of the native structure (*7*). For example, changes in the charge distribution caused by a pH change may even lead to the unfolding of the native state (*8*). Knowledge of the electrostatic interactions in a protein at the microscopic level is crucial to understanding its biological behavior and to designing its rational modification. This requires the knowledge of individual pK_a values for each ionizable amino acid side chain. NMR[1] spectroscopy is a powerful technique for this purpose since individual pK_a values can be determined on the basis of chemical shift changes as a function of pH. Although the determination of ionization constants of histidine residues was an early application of NMR spectroscopy for the understanding of enzyme ligand binding and catalysis (*9*−*11*), only for a few proteins have all pK_a values in the range of 1−8 been fully characterized, probably because of the significant effort required (*12*−*19*). Characterization of the electrostatic

† This work was supported by the Dirección General de Investigación Científica y Técnica (Spain) (PB93-0189) and by the Dirección General de Enseñanza Superior (Spain) (PB96-0601). J.L. is a recipient of a fellowship from the Fundación Ferrer (Barcelona).

* Corresponding author: Instituto de Estructura de la Materia, Consejo Superior de Investigaciones Científicas, Serrano 119, 28006 Madrid, Spain. Fax: 34 91 564 24 31. E-mail: rico@malika.iem.csic.es.

‡ Consejo Superior de Investigaciones Científicas.

§ Present address: Howard Hughes Medical Institute, University of Maryland Baltimore County, 1000 Hilltop Circle, Baltimore, MD 21250.

|| Universidad Complutense.

[1] Abbreviations: NMR, nuclear magnetic resonance; WATERGATE, water suppression by gradient-tailored excitation; TSP, (trimethylsilyl)-propionic acid; COSY, correlated spectroscopy; TOCSY, total correlated spectroscopy; NOESY, nuclear Overhauser enhancement spectroscopy; ApA, adenosyl(3′−5′)adenosine; EDTA, ethylenediaminetetraacetic acid; 2′-GMP, guanosine 2′-phosphate; 3′-GMP, guanosine 3′-phosphate; HPLC, high-performance liquid chromatography; GpA, guanylyl-(3′−5′)adenosine; CD, circular dichroism; RNase, ribonuclease.

10.1021/bi981672t CCC: $15.00
Published on Web 10/22/1998

properties of proteins can be a great help in the elaboration of mechanistic descriptions of substrate recognition processes (*15*, *20*) and catalysis (*16*). In this regard, the measurement of pK_a values for residues directly involved in catalysis, combined with an analysis of the pH dependence of enzymatic activity, will most certainly provide key insights.

This study is focused on α-sarcin, a cytotoxin produced by the mold *Aspergillus giganteus*. It is a small (150 residues) ribosome-inactivating protein that inhibits protein biosynthesis by cleaving a single phosphodiester bond in a strictly conserved sequence of the largest rRNA (*21*) subunit. The protein must be able to enter cells to exert its ribonucleolytic action on the ribosome (*22*). α-Sarcin is the most representative member of a distinctive family of fungal ribonucleases, related to the RNase T1 subfamily, but with differential characteristics, namely, its exquisite substrate specificity and the ability to interact with and translocate across phospholipid bilayers (*23*). On the basis of the global three-dimensional structure of the protein, we have proposed that the mechanism of RNA hydrolysis by the α-sarcin family of proteins should be very similar to that of RNase T1 (*24*). A distinctive feature of the α-sarcin structure, as compared with RNase T1-like proteins, is the presence of large and flexible loops connecting regular secondary structure elements. It has been suggested that these loops account for the specific properties of α-sarcin. Two positively charged loops, which flank the entrance to the active site (loops 2 and 3), are believed to interact with the target rRNA by forming salt bridges with the negatively charged phosphates of the substrate. The protein loops may also account for the observed in vitro interaction with negatively charged bilayers (*25*, *26*), which may help α-sarcin enter the cell. A complete characterization of the electrostatic behavior of this protein is therefore of great interest for a better understanding of all these fundamental processes.

In this work, the individual pK_a values of a large number of ionizable groups in the pH range of 3.0−8.5 have been determined, and those participating in bonding and catalysis were examined in the absence and in the presence of an inhibitor. This work relies on the previous ^{1}H resonance assignments (*27*) as well as on the determined solution structure (*24*). Data from two-dimensional ^{1}H NMR experiments were collected as a function of pH, and the titration curves for a large number of proton resonances were analyzed by nonlinear least-squares fitting to simple ionization models. The calculated pK_a values are discussed in light of the structural environment of the ionizable side chains. Finally, the determined pK_a values of the catalytic residues have allowed a meaningful analysis of the pH dependence of the enzyme activity, leading to a detailed understanding of the ribonucleolytic mechanism of α-sarcin.

EXPERIMENTAL PROCEDURES

Enzyme Activity Assay. The enzymatic activity of α-sarcin has been measured by using ApA as a substrate (*28*) in either 50 mM sodium phosphate or acetate buffers, containing 0.1 M NaCl and 5 mM EDTA. A combination of both buffers allowed us to study the pH dependence of enzyme activity within a wide pH range (2.5−8.5). The extent of adenosine production was measured to evaluate the activity of the protein. The observed pH dependence of the α-sarcin activity was fit to a model involving two mechanisms that share a common residue. The fitting was carried out by a nonlinear least-squares regression analysis using the following equation:

$$\frac{k_{cat}}{K_M} = \frac{A}{1 + 10^{(pK_I - pH)} + 10^{(pH - pK_{II})}} + \frac{B}{1 + 10^{(pK_{II} - pH)} + 10^{(pH - pK_{III})}} \quad (1)$$

In eq 1, pK_I, pK_{II}, and pK_{III} are the pK_a values of the residues in the mechanisms considered and A and B are the relative contributions of the two mechanisms. Most of the parameters of the above model are strongly correlated to each other, making their independent determination and the assessment of errors difficult. Therefore, a grid search was performed, where A and B were systematically varied in steps of 1 unit over the ranges of 100−120 and 30−65 (respectively) and the parameters pK_I, pK_{II}, and pK_{III} were fitted with eq 1 for a minimal χ^2 at each A/B pair. Those fits whose χ^2 values were less than twice that of the best fit (A = 110 and B = 33), were judged to be well-converged. Then, we define the confidence interval for each parameter (pK_I, pK_{II}, and pK_{III}) as the range between their maximum and minimum value from the set of well-converged fits.

NMR Samples. α-Sarcin was prepared and used for NMR spectroscopy as described previously (*24*, *27*, *29*). Unlabeled samples for NMR experiments were prepared at a concentration of 2 mM, in either D_2O or 90% H_2O/10% D_2O containing 0.2 M NaCl. The pH was adjusted to the required values by adding appropriate amounts of concentrated HCl or NaOH (pH measurements were not corrected for isotope effects). Sodium trimethylsilyl(2,2,3,3-$^2H_4$)propionate was used as an internal reference (*30*). All spectra were acquired on a Bruker AMX-600 spectrometer at 308 K. Time-proportional phase incrementation was used for quadrature detection in the indirect dimension (*31*). Water suppression was achieved by selective presaturation of the water signal or by including the WATERGATE module (*32*) in the original pulse sequences. ^{1}H homonuclear COSY (*33*), TOCSY (*34*), and NOESY (*35*) spectra with mixing times of 50 ms were recorded using standard pulse sequences.

α-Sarcin−2′-GMP and α-sarcin−3′-GMP complexes were prepared by mixing the protein and the mononucleotide to achieve complete protein saturation (molar ratio of 1:2). Spectra of the complexes were recorded under the same conditions as those of the free protein, and the assignment was carried out by the standard NOE-based methodology (*36*). The NMR spectra of the α-sarcin−3′-GMP complex were not used for the analysis because relatively high amounts of nucleotide degradation products were detected even after a short period of time. The assignment of the α-sarcin−2′-GMP complex spectrum was assisted by comparison with the spectra of free α-sarcin (*27*).

pH Titrations. The effect of pH titration on the chemical shifts of protons in the free enzyme was determined by analyzing a series of TOCSY and NOESY spectra recorded at different pH values ranging from 3.0 to 8.5. Out of this pH range, denaturation occurs at the concentrations of the protein employed. pH-dependent shifts of protons in the TSP reference were corrected as described previously (*37*, *38*).

Measurements of the pH sample between 3.0 and 8.5 at intervals of 0.5 pH unit were taken at room temperature before and immediately after the NMR experiment. For most resonances, the chemical shift differences between the consecutive spectra were small and allowed the facile assignment by comparison with the assigned spectra under the reference conditions (*27*). All two-dimensional spectra were analyzed on an IRIS Indigo workstation using version 3.3 of the program ANSIG (*39*, *40*).

For the α-sarcin−2′-GMP complex, a set of one-dimensional NMR spectra in D_2O, recorded under the same conditions as those employed for the free protein, was used for the analysis of the histidine ionization constants. Ambiguities were solved with the help of two-dimensional TOCSY spectra recorded at pH 3.0, 4.0, 5.0, 6.5, 7.5, and 8.5.

Calculation of the pK_a Values. pK_a values were determined by measuring the changes in the ^{1}H resonances of the protein as a function of pH. When possible, the pK_a values were calculated by a nonlinear least-squares fit of the experimental pH titration curves to the following equation:

$$\delta_{obs} = \frac{\delta_1 + \delta_2 \times 10^{(pH-pK_I)}}{1 + 10^{(pH-pK_I)}} \quad (2)$$

This equation considers the titration of one group. δ_1 and δ_2 represent the chemical shift values at the low and high extremes of pH, respectively. For situations where more than one titrating group is potentially involved, fits were made to the simple expression (eq 3), corresponding to the noninteracting model.

$$\delta_{obs} = \frac{\delta_1 + \delta_2 \times 10^{(pH-pK_I)} + \delta_3 \times 10^{(2\times pH-pK_I-pK_{II})}}{1 + 10^{(pH-pK_I)} + 10^{(2\times pH-pK_I-pK_{II})}} \quad (3)$$

In eq 3, δ_1−δ_3 represent the individual chemical shift values of the observed resonance in the different protonation states. Equations 2 and 3 were derived from the Henderson−Hasselbach equation assuming a rapid equilibrium between protonated and unprotonated forms (*13*).

In some cases, when two or more titrating groups are close in the three-dimensional structure, we have tried to fit the data to an interacting model (*41*). This model involves a higher number of variables, which in addition are strongly correlated, which is what makes their determination difficult. Nevertheless, tests were carried out to determine if the interacting model could improve the fitting of the experimental titration data. The approach resulted in a poor determination of the additional parameters without improving substantially the fitting. This led us to apply a noninteracting model in all cases.

Only resonances assigned under all experimental conditions were used for the analysis; resonances displaying small chemical shift changes (typically less than 0.08 ppm) were regarded as pH-independent. Using these criteria, 209 titration curves were fitted to eq 2 or 3 to obtain statistically significant titration parameters.

The pK_a of a given ionizable group is determined from the chemical shift variation (titration curve) of protons chemically close to the titrating group. In addition to these protons, we may find others, belonging to residues spatially close to the titrating group, whose chemical shifts may be affected by its ionization state so that their titration curves would also reflect the pK_a of that group. In fact, it was found that in many cases the ionization of the titrating group affected not only the chemical shifts of protons in its side chain but also those of protons in nearby residues. In these cases, the pK_a was calculated as the weighted average of those resulting from the analysis of the various titration curves. Since large titration shifts yield more accurate pK_a values, the magnitude of the chemical shift change was used as the weighting factor for the determination of the averaged pK_a. The error obtained from each pK_a value was used to calculate the standard error.

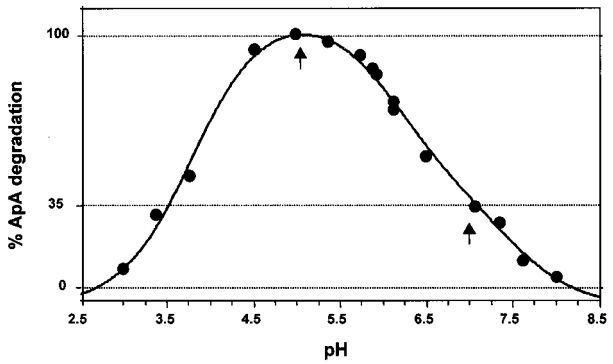

FIGURE 1: Effect of pH on the ApA degradation by α-sarcin at 25 °C. Activity values are expressed in terms of adenosine production, considering the value obtained at pH 5.0 as 100%. The continuous line represents the best fit of the experimental results, corresponding to two ribonucleolytic mechanisms and three ionizable groups with apparent pK_a values of 3.7, 6.2, and 7.7. Arrows indicate the two activity maxima, the main at pH 5.0 and the secondary at pH 7.0.

In the case of the 2′-GMP−α-sarcin complex, the individual pK_a values were calculated from chemical shift changes upon pH titration of the Hϵ_1 and Hδ_2 His proton resonances in the one-dimensional ^{1}H NMR spectra. These sets of data were fitted to eq 2 or 3, and the standard error for each fitting parameter was computed from the diagonal elements of the variance−covariance matrix.

All reported standard errors reflect the precision of the data fitting and do not include the uncertainty in the pH determination of the sample, which is estimated to be ±0.1 unit.

RESULTS

Enzymatic Analysis. Quantitative measurements of the ribonucleolytic activity of α-sarcin have been impaired by the absence of a convenient assay. Recently, an evaluation of the α-sarcin activity has been described, consisting of measuring the products resulting from the hydrolysis of ApA or GpA after HPLC separation (*28*). This assay has now been used to study the effect of pH on the enzymatic activity of α-sarcin (Figure 1). The resulting plot clearly shows that α-sarcin behaves as an acid ribonuclease, with an optimum pH of 5.0, and an activity at neutral pH of about 30% of the maximum value. These results have been analyzed according to several models involving two or three catalytic residues as well as one or two hydrolysis mechanisms. The best fit has been obtained for a model composed of two mechanisms involving three residues, one of each being common to both mechanisms (eq 1). The pK_a values of these three residues were 3.7, 6.2, and 7.8. The first mechanism accounts for

Table 1: Chemical Shifts[a] and Chemical Shift Variations (parts per million) upon Complex Formation for His Resonances of α-Sarcin (H_2O) and the α-Sarcin−2′-GMP Complex (D_2O) at pH 4.0, 35 °C, and 0.2 M NaCl

	α-sarcin		α-sarcin−2′-GMP complex		$\Delta\delta = \delta_{complex} - \delta_{free}$	
residue	Hϵ_1	Hδ_2	Hϵ_1	Hδ_2	Hϵ_1	Hδ_2
His35	8.72	7.06	8.73	7.03	0.01	−0.03
His36	8.70	7.35	8.71	7.31	0.01	−0.04
His50	8.11	7.18	8.22	7.05	0.11	−0.13
His82	8.05	3.50	8.02	3.47	−0.03	−0.03
His92	8.93	7.65	8.90	7.63	−0.03	−0.02
His104	6.73	7.02	6.68	7.00	−0.05	−0.02
His137	8.98	7.19	8.87	7.05	−0.11	−0.14
His150	8.88	6.23	8.85	6.22	−0.03	−0.01

[a] Not corrected for isotope effects.

the maximum at pH 5.0 and would involve two catalytic residues with pK_a values of 3.7 and 6.2 acting as a general base and acid, respectively. The second mechanism, responsible for the shoulder at pH 7.0, would involve the residue with a pK_a of 6.2 as a general base, and the third residue with a pK_a of 7.8 acting as an acid. No activity was detected below pH 2.5 or above pH 8.5. This is consistent with fluorescence and circular dichroism studies (*42*). The protein is unfolded below pH 2.5, and partially denaturated above pH 8.5, whereas the spectroscopic properties of α-sarcin remained unaltered in the pH range of 2.5−8.5.

NMR Assignments. Nearly complete ^{1}H and ^{15}N NMR resonance assignments for α-sarcin have been previously reported (*27*). Here we have extended the ^{1}H resonance assignment on the basis of intraresidue scalar connectivities together with short- and long-range NOE effects. With this analysis, many protons from prolines and long side chain residues could be assigned. All of these assignments, at pH 4.0 and 308 K, have been deposited at BioMagResBank (http://www.bmrb.wisc.edu/) under accession number 4158.

Resonances for most of the protons in the α-sarcin−2′-GMP complex were also assigned at pH 4.0, 5.5, 6.0, 7.0, 7.9, and 8.5 by standard NOE-based methodology (*36*) and by comparison with the free protein data. The observation of intranucleotide NOEs with the same sign as the protein signals (as opposed to different sign of intranucleotide NOEs for the free nucleotide), and the detection of changes in the chemical shifts of several protein protons in the presence of the nucleotide (*43*), indicate in an independent way that the protein−nucleotide complex has been formed under our experimental conditions.

Special attention was paid to the unambiguous assignment of the histidine aromatic protons in the complex. The chemical shifts of the histidine resonances in the complex and the differences with corresponding protons in the free enzyme are reported in Table 1. The anomalous chemical shift of Hδ_2 of His82 is explained by the proximity of this aromatic proton to the Trp51 aromatic ring. In addition, the chemical shift value of His104 Hϵ_1 is perturbed due to its proximity to Phe100 (*24*).

Chemical shift changes reveal that only His50 and His137 are sensitive to complex formation (Table 1). Both nonexchangeable aromatic protons, Hϵ_1 and Hδ_2, of these residues located in the active center display significant changes upon complex formation (larger that 0.1 ppm). This is in agreement with that observed for other enzyme−substrate complexes studied by NMR where only the chemical shifts of protons in a small fraction of the residues of the protein are affected by the binding, those being at or near the active site, as reported for RNase A (*44*) and RNase T1 (*45*).

Titration of Ionizable Groups of α*-Sarcin*. Analysis of a large amount of data collected for the ribonuclease α-sarcin yields a total of 670 unambiguously assigned protons studied at all pHs. The largest titration shift within the experimental pH range is that of His137 Hϵ_1 ($\Delta\delta$ = 1.26 ppm). Some other protons also showing high values for $\Delta\delta$ are mainly backbone or side chain amide. In fact, from the 15 protons that have markedly large titration shifts, eight are NH protons (Lys11 HN, Lys61 HN, Asn12 Hδ_{21}, Gly45 HN, Asn54 HN, Asp59 HN, Gln27 Hϵ_{21}, and His150 HN). This indicates, as expected (*13*), that the amide proton chemical shifts are most sensitive to environment because N−H bonds are more polarizable that C−H bonds. While the three-dimensional solution structure of α-sarcin has not yet been completely refined, all present data indicate that the NHs with large $\Delta\delta$ are H-bond donors to side chain carboxylate groups (*24*). Such H-bonds are observed for homologous NH groups in the recently published crystal structure of restrictocin (*46*), a protein closely related in terms of primary structure and function to α-sarcin (*22*).

On the other hand, the magnitudes of the largest titration shifts for CH protons are, in general, lower than that for NH protons. Such CH protons belong to titrating side chain groups of His137, His50, Glu144, Asp59, His35, His92, and Asp57 or are close to them (Lys81, Thr125, Leu145, Gln142, and Asn128). This last group corresponds to residues located in the protein interior.

Determination of pK_a Values of the Ionizable Groups of the α*-Sarcin.* pK_a values were determined from titration curves of protons with a significant titration shift over the entire pH range and showing a good fit (correlation coefficient > 0.99) to the models described by eq 2 or 3. Two hundred nine titration curves match these criteria and correspond to protons homogeneously distributed all over the protein structure. Typical proton titration curves for free α-sarcin are shown in Figure 2.

On the basis of the nominal pK_a values of ionizable side chain groups (*47*), a total number of 27 groups are expected to titrate within the experimental pH range considered. These are 11 aspartic acid residues (Asp9, Asp41, Asp57, Asp59, Asp75, Asp77, Asp85, Asp91, Asp102, Asp105, and Asp109), six glutamic acid residues (Glu19, Glu31, Glu96, Glu115, Glu140, and Glu144), the C-terminal carboxylate, eight histidine residues (His35, His36, His50, His82, His92, His104, His137, and His150), and the N-terminal amino group. The location of these titrating groups in the α-sarcin structure is shown in Figure 3. The pK_a values of the ionizable groups mentioned above and determined in this work are summarized in Table 2. In this table, two sets of experimental pK_a values are given. The first set (pK_a intra) is obtained by considering only the chemical shift changes of protons belonging to the side chain of the same residue. The second set (pK_a weight) is the weighted average of pK_a values determined for all protons whose chemical shift are sensitive to the titration of the corresponding ionizable group (see Experimental Procedures). The pK_a values calculated from the two different strategies (only intraresidual values vs intra- and interresidual values) show excellent agreement. The obtained pK_a values are compared in Table 2 with the

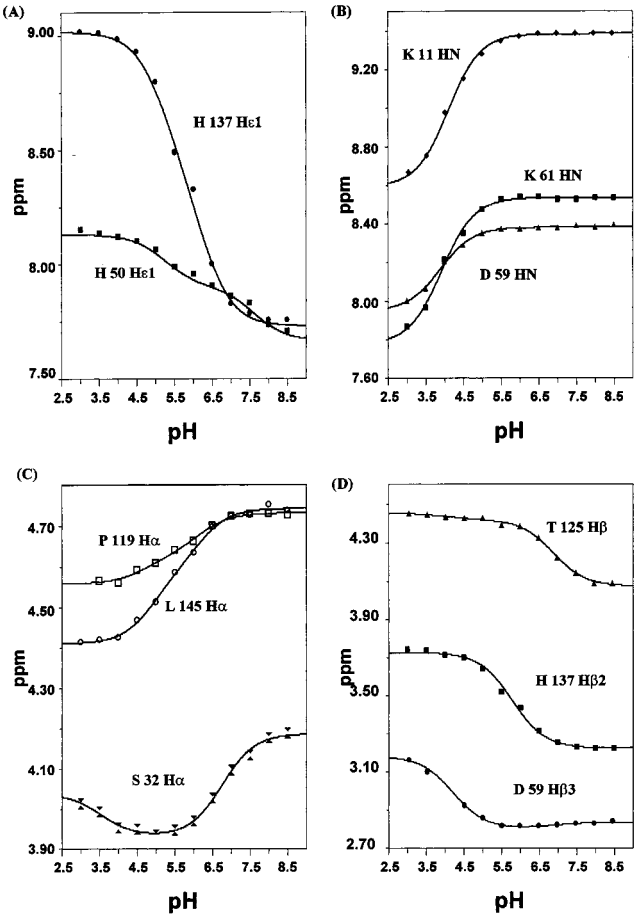

FIGURE 2: Chemical shift titration curves for several proton resonances of free α-sarcin in the pH range of 3.0−8.5. Data points were taken from NOESY spectra. The solid line is the least-squares best fit to the data. The pK_a values determined from fitting the data to eq 2 or 3 are listed in Table 2: (A) titration of Hϵ_1 protons of His137 and His50, (B) titration of NH protons of Lys11, Lys61, and Asp59, (C) titration of Hα protons of Pro119, Leu145, and Ser32, and (D) titration of Hβ protons of Thr125, His137, and Asp59.

intrinsic values of the titrating groups reported in the literature (*47*). Out of the 209 titration curves which fit model 2 or 3, we could identify unambiguously the titrating groups causing the change in the chemical shift in 154 cases (third column in Table 2), and these 154 curves were used to calculate the pK_a values given in Table 2. We have, however, more confidence in the weighted averaged values since these pK_a values are based on more data. For this reason, we have used these values in the subsequent analysis.

Now, we will describe the results of the pK_a determination in detail. On the basis of spatial proximity (Figure 3), the ionizable side chains can be considered as belonging to six different groups which are relatively isolated from each other. The first set of titrating residues (group I) is comprised of His150, and the N and C termini of the protein. The pK_a of the C-terminal carboxylate was easily determined by following chemical shift changes in Thr5 HN, His150 HN, His150 Hα, His150 Hβ_2, and His150 Hβ_3 curves which provide a value of 3.5 ± 0.1. It was difficult to determine unambiguously the pK_a of His150 in the free protein. His150 Hϵ_1 and Hδ_2 data could not be accurately fit to equation models, which prevented the calculation of the pK_a using the imidazolium resonances. For this reason, the His150 pK_a was obtained from chemical shift changes of nearby protons. While the histidine amide HN has an apparent pK_a of 7.5, this value could not be, however, assigned unequivocally to either the N-terminal NH_3 or the His150 ring since it is close

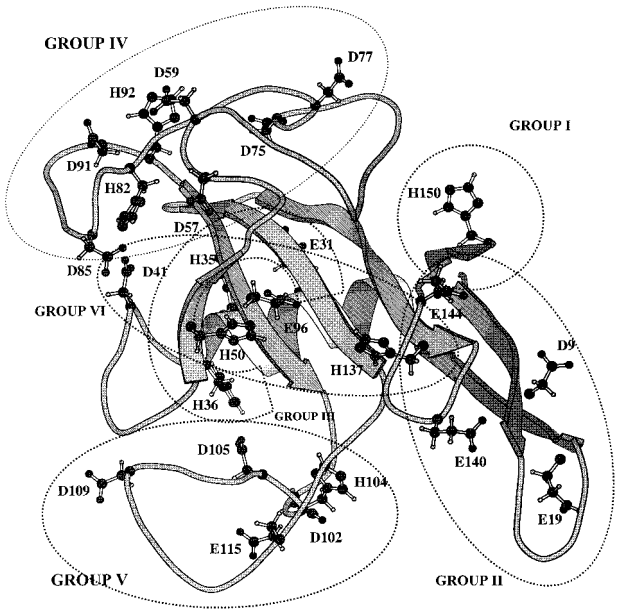

FIGURE 3: Ribbon representation of the solution structure of α-sarcin (*24*) illustrating the location of the potentially titrating groups (Asp, Glu, and His) in the pH range of 3.0−8.5 and the six groups (I−VI) considered on the basis of spatial proximity. The ribbon drawing was created with the program MOLSCRIPT (*77*).

Table 2: pK_a Values of α-Sarcin Ionizable Groups Measured by NMR in H_2O at 308 K in the pH Range of 3.0−8.5

	p$K_{a-intra}$[a]	p$K_{a-weight}$[b]	no. of protons[c]	p$K_{a-intrinsic}$[d]	group
C-term	3.6 ± 0.2	3.5 ± 0.1	5	3.6	I
D9	3.9 ± 0.1	3.9 ± 0.1	12	4.0	II
D41	<3	<3		4.0	IVa
D57	4.3 ± 0.1	4.3 ± 0.1	3	4.0	IVa
D59	4.1 ± 0.1	4.0 ± 0.1	10	4.0	IVa
D75	3.9 ± 0.1	3.8 ± 0.1	5	4.0	IVb
D77	<3	<3		4.0	IVb
D85	3.8 ± 0.1	3.8 ± 0.1	2	4.0	IVa
D91	<3	<3		4.0	IVa
D102	<3	<3		4.0	Va
D105	<3	<3		4.0	Va
D109	3.7 ± 0.2	3.7 ± 0.2	6	4.0	Vb
E19	4.6 ± 0.2	4.6 ± 0.2	2	4.5	II
E31	4.6 ± 0.2	4.6 ± 0.2	11	4.5	III
E96	5.1 ± 0.1	5.2 ± 0.1	13	4.5	VI
E115	4.9 ± 0.1	4.8 ± 0.1	5	4.5	Va
E140	4.3 ± 0.1	4.2 ± 0.1	3	4.5	II
E144	4.3 ± 0.1	4.3 ± 0.1	2	4.5	II
H35	6.3 ± 0.1	6.3 ± 0.2	7	6.8	III
H36	6.8 ± 0.1	6.8 ± 0.2	10	6.8	III
H50	7.7 ± 0.2	7.7 ± 0.2	7	6.8	VI
H82	7.3 ± 0.1	7.3 ± 0.1	4	6.8	IVa
H92	6.9 ± 0.1	6.9 ± 0.1	11	6.8	IVa
H104	6.6 ± 0.2	6.5 ± 0.2	4	6.8	Va
H137	5.8 ± 0.1	5.8 ± 0.1	30	6.8	II
H150	7.5 ± 0.2	7.6 ± 0.2	2	6.8	I
N-term	−	−		7.7	I
total			154		

[a] pK_a values calculated by using only intraresidue chemical shift proton pH dependence. [b] Weighted-averaged pK_a values. [c] Number of protons used in the average weighted methodology. [d] Intrinsic pK_a values, expected values in the absence of any influence from the other charged sites of the protein (*47*).

to both these groups. In addition, the Thr5 HN also titrates at around pH 7.8. This proton is hydrogen bonded to the carbonyl oxygen of Ser149 (*24*) and is closer to the His150 side chain than to the N-terminal amino group. It is reasonable to suggest that the titration of the His150 ring affects the chemical shift of both protons (Thr5 HN and His150 HN). Consequently, the pK_a of the aromatic ring is taken as an average of the values reported by these two groups. The pK_a of the N-terminal ammonium group shall lie in the same range as that of His150.

Group II of ionizable residues comprises two acid residues, Asp9 and Glu19, from the N-terminal hairpin, and three residues from the fourth strand of the central β-sheet, Glu140, Glu144, and His137 (Figure 3). The pK_a of Asp9 was easily determined from the chemical shift changes of its own β protons as well as from those of several protons close in the protein structure (Gln10 Hϵ_{21}, Gln10 Hγ_2, Lys11 HN, Lys11 Hα, Asn12 Hδ_{21}, Asn12 Hδ_{22}, Tyr18 Hα, Glu19 HN, Thr20 Hα, and Lys21 HN). Its value, 3.9, is not far from that corresponding to an aspartic acid in unstructured tetrapeptides (*38*). Glu19 is located in the poorly defined and mobile turn of the N-terminal hairpin, and it is highly exposed. Its pK_a value, 4.6, was determined from its β protons, and it is close to the intrinsic value for a glutamic acid. For Glu140 and Glu144, we could measure the corresponding pK_a with chemical shift changes in their γ protons and also in nearby protons (Asn141 Hα for Glu140 and Thr138 HN for Glu144). These two residues show pK_a values which are also close to the intrinsic value (4.3 for Glu140 and and 4.3 for Glu144). His137 is an important residue because it has been proposed to be one of the catalytic residues. The pK_a (5.8) of His137 was cleanly determined from its own Hϵ_1, Hδ_2, and Hβ_2 protons which all show large chemical shift changes upon titration, and from the chemical shift changes in 30 nearby protons, e.g., Asp9 HN, Gln10 Hϵ_{21}, Ile23 HN, Phe52 HN, Pro119 Hα, and Leu147 HN. Many protons are sensitive to the titration of His137 because it lies in the interior of the protein, where the dielectric constant is low.

Glu31, His35, and His36, located in the single α-helix of α-sarcin, form the third group of titrable amino acids. The pK_a values of these residues were calculated from chemical shift changes measured in their own protons together with changes measured in nearby protons, belonging either to the α-helix or to the β-strand on which is packed the α-helix. In the case of Glu31, an average pK_a of 4.6 was obtained from the individual titrations of Gln27 Hβ_2, Gln27 Hϵ_{21}, Gln27 Hϵ_{22}, Lys27 NH, Lys29 HN, Ala30 HN, Glu31 HN, Glu31 Hγ_2, Glu31 Hγ_3, Ser32 HN, and Phe131 Hζ. For His35, protons Ser34 Hγ, His35 HN, His35 Hα, His35 Hβ_2, His35 Hδ_2, Ala130 HN, and Phe131 HN were used to calculate an average pK_a value of 6.3. The last helical residue, His36, has a pK_a of 6.8. This value was determined by monitoring the titration of Ser32 Hα, Gly33 HN, His36 Hα, His36 Hβ_2, His36 Hβ_3, His36 HN, Ala37 Hα, Leu39 Hβ_3, Phe108 Hδs, and Phe108 Hϵs.

Group IV is composed by the titratable side chain groups of amino acids in loop 1 and loop 2. Residues Asp57, Asp59, His82, Asp85, Asp91, and His92 are all located in loop 2, the longest loop in the protein structure (Figure 3). These residues, together with Asp41 which belongs to loop 1, form subgroup IVa. Asp57 and Asp59 are close to the end of the first strand of the central β-sheet. The pK_a values calculated for these aspartic acid residues are 4.3 and 4.0, respectively. Although these aspartates have similar pK_a values, their titrations affect the chemical shifts of two distinct groups of surrounding protons. One group, composed of Tyr56 HN, Asp57 Hβ_2, and Asp57 Hβ_3, is affected by the titration of Asp57. Changes observed in the other group, consisting of protons Tyr56 Hβ_3, Asp57 NH, Gly58 HN, Gly58 Hα_1, Asp59 Hα, Asp59 Hβ_3, Gly60 Hα_1, Lys61 HN, Lys60 Hβ_2, and Leu62 HN, matched very well with the ionization constant of Asp59. This behavior, together with the large chemical shift variations of some of the HN protons in this region (Gly45 HN, Asp59 HN, and Lys61 HN), can only be explained by assuming that this part of the loop has a well-defined structure. His82 has a pK_a value of 7.3, which is slightly higher than that of short peptides (*38*). This value was obtained from the titration of its own protons together with that of the Trp51 Hϵ_1 which lies close to His82. The pK_a of Asp85 was measured only from its β and HN protons, and its value was 3.9. In the case of Asp91, all protons in this residue showed a very small chemical shift variation ($\Delta\delta < 0.04$ ppm) over the entire pH range. That classifies these protons as pH-independent in the studied pH range (as described in Experimental Procedures) and suggests that the pK_a of this aspartate is less than 3.0. His92 shows a more classic behavior. Its pK_a value is 6.9 and was obtained from the titration of 11 nearby protons, including some belonging to residues in the opposite β-sheet strand (Tyr126 HN, Hβ_3, and NH).

Loop 2 also contains aspartic acid residues 75 and 77 (subgroup IVb). The pK_a of Asp75 was determined from the values for Asp75 Hβ_2, Asp75 Hβ_3, Cys76 HN, Asn128 Hδ_{22}, and Phe131 HN, yielding a value of 3.8. The chemical shifts of Asp77 protons do not vary significantly over the pH range studied, suggesting that the pK_a of this residue could be less than 3.0.

The ionizing residues of loop 3 can be split in two groups, Va and Vb. Residues Asp102, His104, Asp105, and Glu115, which form a network of hydrogen bonds within loop 3, comprise the first group. Asp102 and Asp105, like Asp77 and Asp41, show no significant chemical shift change in the acidic region, suggesting that the carboxylate group of these residues titrates below pH 3.0. None of the protons of Asp102 show significant changes in their δ values between pH 3.0 and 8.5, whereas HN and Hβ_3 of Asp105 show significant chemical shift changes only above pH 8.0. The origin of the chemical shift changes above pH 8.0 remains unknown. It may likely correspond to the titration of a nearby group with an abnormally low pK_a, such as that of Lys or Tyr. The absence of data above pH 8.5 precludes the determination of either this pK_a or the residue responsible for it. The pK_a calculated for His104 is 6.5, and its effect was observed in His104 HN, His104 Hδ_2, His104 Hϵ_1, and Lys107 HN. For Glu115, the pK_a was 4.8 and was measured by using the chemical shift changes observed in Glu96 Hβ_3, His104 Hα, Glu115 Hγ_2, Pro119 Hα, and Ala120 Hα.

Asp109 (group Vb) is also part of loop 3, but it does not enter into the hydrogen bonding network. Asp109 has a pK_a of 3.7, as measured from chemical shift changes in its own protons, and in some protons of Phe108 and the HN of Gly45.

Finally, two important ionizable side chain groups, Glu96 and His50 (group VI), lie close to each other deep within

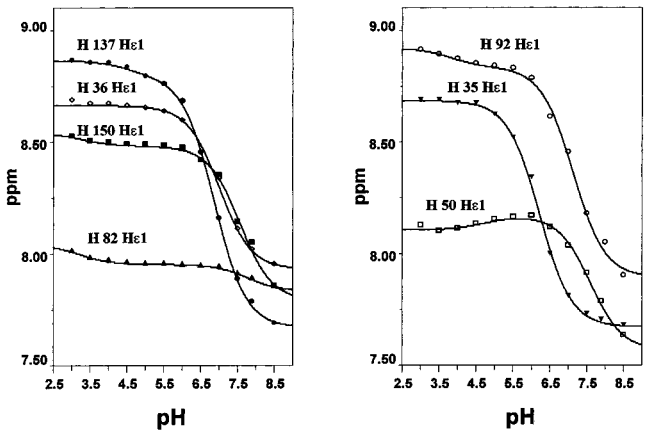

FIGURE 4: Chemical shift titration curves of His Hϵ_1 resonances of the α-sarcin−2′-GMP complex in the pH range of 3.0−8.5. Data points were taken from one-dimensional spectra. The solid line is the least-squares best fit to the data. The pK_a values determined from fitting the data to eq 2 or 3 are listed in Table 3: left, His137, His36, His150, and His82; right, His92, His35, and His50.

the protein structure. These residues have been proposed to be part of the protein active site (*42*). The pK_a of His50 (7.7) is rather higher than the expected value for a histidine, whereas the pK_a of Glu96 has a value of 5.2, which is significantly higher than the one expected for a glutamic acid. As these side chains are located in the core of α-sarcin, their titrations are reflected in the chemical shift changes in many nearby protons that are distributed throughout the protein sequence: Tyr48 HN, His50 Hβ_2, His50 Hβ_3, His50 Hϵ_1, Phe52 Hδs, Gly86 Hα_2, and Glu96 HN for His 50 and Phe52 Hα, Phe52 Hζ, Asn54 HN, Glu96 Hα, Glu96 Hγ_2, Arg121 HN, Val122 HN, Ile123 NH, Ile123 Meδ_1, Ile123 Meγ_2, Ile135 Meδ_1, Gly143 Hα_1, Leu145 Hα, and Leu145 Hβ for Glu96.

Determination of pK_a Values of Histidine Residues in the α-Sarcin−2′-GMP Complex. A set of one-dimensional ^{1}H NMR spectra recorded in D_2O over the complete pH range considered was used to determine the histidine ionization constants in the α-sarcin−2′-GMP complex. To that end, we measured the pH dependence of the chemical shifts of the Hϵ_1 and Hδ_2 histidine protons. Only the proton resonances that could be followed unambiguously over the entire pH range were used for the pK_a determination. The data were fitted to models of one or two noninteracting pK_a values (eq 2 or 3). All pK_a values could be determined accurately from signals that had large chemical shift changes (from 0.5 to 1.0 ppm) with little scatter, except for His82. Curves corresponding to these fits are shown in Figure 4. Table 3 shows the pK_a of His residues for both free and complexed enzyme determined from H_2O and D_2O data, respectively. In the acidic pH range, the pK_a values determined in D_2O are approximately 0.06 pH unit higher than the corresponding pK_a in H_2O, whereas in the basic pH range, the pK_a values in D_2O are approximately 0.1 unit higher than that in H_2O (*38*). Large differences in the pK_a values between free and complexed enzyme, not imputable to the solvent effect, are observed for His137 and His82 and probably for Glu96. His137 and Glu96 have been proposed to be the catalytic residues in α-sarcin by comparison with the RNase T1.

His35 and His36, both in the α-helix, show almost the same chemical shift values for protons Hδ_2 and Hϵ_1 in the 2′-GMP−sarcin complex as in the free enzyme (Table 1). Hϵ_1 titration data for both His35 and His36 show a single titration curve, and the corresponding pK_a values are 6.2 and 7.0, respectively. A pK_a value of 7.1 for His92 was calculated from the pH titration of its own Hϵ_1. Chemical shifts of the Hϵ_1 and Hδ_2 protons in the complex are also close to those measured in the free enzyme (Table 1). The C-terminal residue, His150, shows an unaltered electrostatic behavior in the complex as compared to the free enzyme. Its Hϵ_1 and Hδ_2 protons can be observed over the whole experimental pH range, and the pK_a was calculated from titration curves of both protons, giving values of 7.5 and 7.4. These values agree with each other and are close to the pK_a of the free enzyme. Unfortunately, the determination of the pK_a of His104 was hindered by spectral overlap.

Table 3: pK_a Values Derived from NMR Measurements of Histidine Residues and Glutamic Acid 96 of α-Sarcin in H_2O and the α-Sarcin−2′-GMP Complex in D_2O[a]

residue	α-sarcin	α-sarcin−2′-GMP complex
His35	6.3 ± 0.2	6.2 ± 0.1
His36	6.8 ± 0.2	7.0 ± 0.1
His50	7.7 ± 0.2	7.6 ± 0.2
His82	7.3 ± 0.1	7.8 ± 1.1
His92	6.9 ± 0.1	7.1 ± 0.1
His104	6.5 ± 0.2	nd[c]
His137	5.8 ± 0.1	6.8 ± 0.1
His150[b]	7.6 ± 0.1	7.5 ± 0.3
Glu96	5.2 ± 0.1	∼4.8[d]

[a] Not corrected for isotope effects. [b] May be coincident with the N-terminal amine ionization. [c] nd, not determined due to the impossibility of following the signals unambiguously by one-dimensional NMR. [d] Indirectly determined from the Hϵ_1 His50 titration curve.

The pK_a of His50, 7.6, was determined on the basis of the titration of its Hϵ_1 proton, and it is close to the value obtained in the free enzyme. In addition, the titration of His50 showed a second, low-pH transition (apparent pK_a of 4.8). It likely reflects the ionization of Glu96 in the complex since in the free enzyme the low-pH titration of His50 is also observed and assigned to Glu96. However, the small magnitude of this chemical shift change ($\Delta\delta = 0.06$) leads us to consider this pK_a value as approximated.

His82 has a pK_a of 7.8, which appears to be ∼0.5 unit higher than its pK_a in the free enzyme. Nevertheless, due to the low accuracy of this determination, it cannot be concluded that the pK_a change was significant. The chemical shifts of the aromatic protons of His82 do not change significantly upon 2′-GMP binding (Table 1). Moreover, the location of His82 far away from the catalytic center suggests that the 0.5 unit difference in the pK_a value, if significant, is not related to 2′-GMP binding.

Large changes in the pK_a and chemical shift values of His137 occur upon 2′-GMP binding. The pK_a, calculated from the dependence of its Hϵ_1 proton resonance with the pH, increases to 6.8 (1.0 pK_a unit greater than in free enzyme). Upon nucleotide binding, the aromatic protons display an upfield shift similar in magnitude to the downfield shifts observed for the His50 Hϵ_1 and Hδ_2 protons. These data indicate that His137 is strongly affected by 2′-GMP binding.

Protons of the 2′-GMP inhibitor also show some chemical shift changes when the pH is altered. Since both free and bound molecules contribute to the observed resonance, only

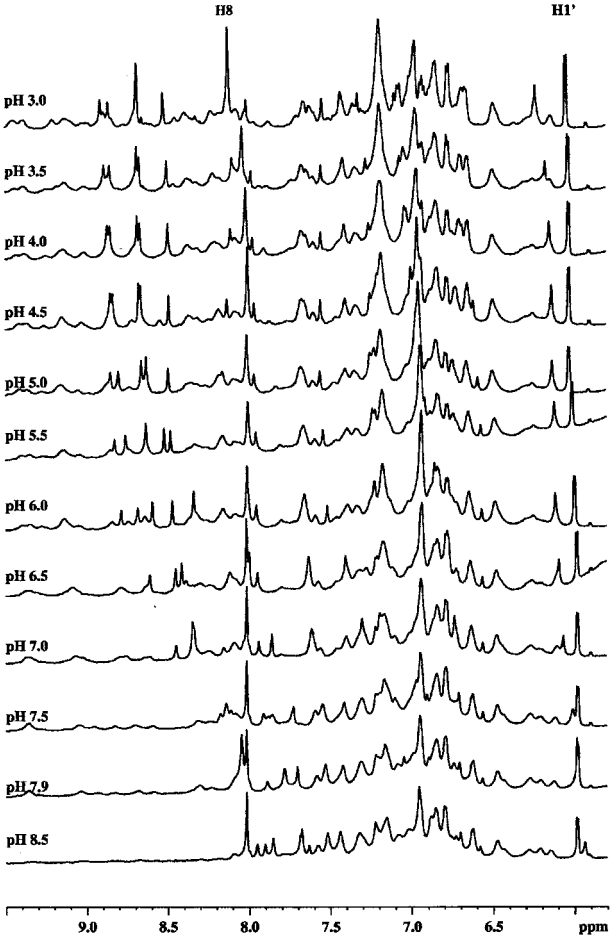

FIGURE 5: Aromatic region of the proton spectra of α-sarcin−2′GMP (1:2) at various pH values in D_2O and at 308 K.

a qualitative interpretation of the 2′-GMP chemical shift changes with pH can be made. Nevertheless, it is possible to observe that the chemical shift of the guanine H_8 resonance is constant between pH 8.5 and 4.0 (Figure 5, bottom to top) but changes significantly below pH 4.0. This change may be due either to the influence of the nucleotide phosphate ionization or to the proximity of an acidic residue in the protein to H_8. The chemical shift of the H_1' of the ribose ring also shows some variation around pH 5.0, a value that could be attributed to the titration of a glutamic acid in the protein.

DISCUSSION

Structural and Electrostatic Determinants of the pK_a Values of Residues in α-Sarcin. Ionizable groups in side chains of amino acids have intrinsic pK_a values (*48*). Changes in these intrinsic values result either from structural interactions (mainly hydrogen bonds and salt bridges) or from the presence of charges in an environment with a low dielectric constant such as the core regions of globular proteins. In practice, titration data from folded proteins show that the majority of the pK_a changes (relative to those the isolated amino acids) (*3*) are relatively small, although in some special cases the pK_a values can be highly perturbed. These deviations can be rationalized in light of the three-dimensional structure, and their energetic contributions to the protein stability can be quantified. With the exception of certain loops, the three-dimensional structure of α-sarcin in aqueous solution is sufficiently well resolved to carry out this analysis (*24*). Figure 3 shows the ionizable side chains of α-sarcin distributed throughout the three-dimensional structure. Most of these side chains are, as expected, surface-exposed and accessible to water molecules as well as solvent ions, and only a small number of titrating side chain groups are located in the protein interior.

We will comment first about those residues which have pK_a values close to those observed in nonstructured peptides (see Table 2). Residues Asp9, Glu19, Glu31, Asp57, Asp59, Asp75, Asp85, Asp109, Glu140, and Glu 144 exhibit pK_a values close to those measured in unstructured peptides for aspartic acid (4.0) and glutamic acid (4.5), respectively. In a similar fashion, His35, His36, His92, and His104 also show pK_a values near that found for a histidine residue in an unstructured peptide (6.8). These data indicate that these residues are not strongly involved in noncovalent interactions and that they contribute little to stabilize the structure. These residues are distributed all over the protein surface and surely contribute to its solubility.

A large number of residues in α-sarcin have pK_a values far from their intrinsic values. These are Asp41, His50, Asp77, His82, Asp91, Glu96, Asp102, Asp105, Glu115, His137, and His150. Interestingly, catalytic residues are included in this second group. In some cases, especially for residues located in poorly defined loops, it is difficult to carry out an accurate analysis of their altered pK_a in structural terms, but some insights can be obtained. Asp41 has a pK_a out of the experimental pH range, and its value is probably less than 3.0. This residue is located on loop 1 (*24*), and it is spatially close to the imidazole group of His82. It seems then reasonable to assume the existence of an interaction between the side chains of Asp41 and His82, which is confirmed by the uncompleted acid titration shown by protons $H\epsilon_1$ and $H\delta_2$ in addition to its own basic pK_a titration. This interaction would fix two of the longer loops in the molecule (loop 1 and loop 2) and thus help to maintain in an efficient way the protein structure. An analysis of the α-sarcin backbone dynamics on the basis of ^{15}N relaxation data (unpublished results) indicates that the local flexibility in these loops is not homogeneous (*49*) but rather that there are some rigid segments as judged by the ^{15}N order parameter values and the protection against exchange of some the involved amide protons. A salt bridge from Asp^-41 to His^+82 would contribute to partially fixing the loop segments in which these residues are inserted. In addition, the imidazole ring of His82 is stacked on the Trp51 indole ring. This kind of interaction is favored by a positive charge in the His ring (*50*, *51*) and contributes, as has been observed, to the shift of its pK_a value to a higher value.

As mentioned, side chains of amino acid residues 41, 77, 91, 102, and 105 (all located in loop regions) show pK_a values lower than 3.0. In a previous study on the effect of pH on α-sarcin stability, the two denaturating transitions were proposed to occur at pH 2.5 and 10.2 (*42*). The first of them is clearly related to one or more of the above residues. Therefore, some or all of these acid side chains are involved in crucial interactions that contribute to the protein stability and maintain the protein fold. In fact, in the crystal structure of restrictocin (*46*), all homologous side chain groups were found to be involved in electrostatic interactions or hydrogen bonds. These interactions are formed mainly by residues

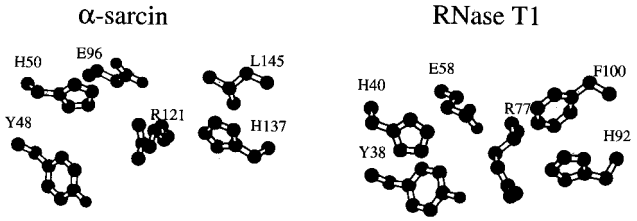

FIGURE 6: Comparison of α-sarcin and RNase T1 active sites. The side chains of the catalytic and nearby residues are shown in the same orientation. Coordinates of RNase T1 were taken from the PDB coordinate file 1YGW (*78*).

that are both in the same loop region. This is the case of those involving Asp76, Asp90, and Asp101 (homologous to Asp77, Asp91, and Asp102 in α-sarcin). However, the interactions involving side chains of residues far away in the sequence are far more interesting because of their relevance in terms of folding and stability. One of these is the one between Asp40 and His81, homologous to that between Asp41 and His82 in α-sarcin described above. Another one is that established between the side chains of residues Asp104 and Asn32 (homologous to that between Asp105 and Asn33 in α-sarcin) that join the first part of loop 3 and the α-helix.

Loop 3 (residues Thr99−Pro119) has the highest concentration of charged residues. The lysine residues of loop 3 (Lys107, Lys111, Lys112, and Lys114) together with Lys43 in loop 1 have been proposed to interact with the negative phosphodiester groups in the ribosomic RNA (*52*). Such a binding could possibly trigger in turn the rearrangement of the loop structures, allowing some of the aspartic acid side chains mentioned above to interact with the base that is crucial for recognition, G10 (*53*). In fact, in the model structure for the interaction of α-sarcin with its RNA substrate (*49*), these two loops contact base G10, which is six residues away from the scissile bond. This type of interaction between Asp and guanine base moieties has been found in several GTPases, like elongation factors, members of the p21-ras family, and G proteins (*54*).

His150, the C-terminal residue, is spatially close to the N terminus in the protein structure and shows a pK_a that is 1 unit higher (7.6) than the intrinsic value. Interaction of His150 with a group near the C or N terminus causes the perturbation of its pK_a. Interaction with an N-terminal residue would assist the 6−148 disulfide bridge in maintaining the relative orientation between the N-terminal hairpin and the central β-sheet.

The pK_a values of α-sarcin catalytic residues deserve special attention. In many proteins, the catalytic residues are somewhat protected in the hydrophobic core. The limited accessibility of the solvent and the low dielectric constant of this region discourage charge formation, and tend to shift the pK_a of Asp and Glu to higher values, and those of His to lower values (*55*). In the solution structure of α-sarcin, the internal pocket is well-defined and provides the structural basis for understanding the electrostatic behavior of these residues. An inspection of the spatial arrangement of the catalytic center (Figure 6) points to an interaction between His50 and Glu96. Both side chains are close, and NOEs between Glu96 Hγ_2−His50 Hδ_2 and Glu96 Hγ_3−His 50 Hδ_2 have been detected. Moreover, the Glu96 titration can be monitored in the chemical shift changes of His50 Hδ_2 and Hϵ_1. Finally, a hydrogen bond links Hδ_1 of His50 to the Glu96 CO backbone in most calculated solution structures. This interaction was detected from the first steps of the solution structure calculations, where only the strongest structural features are generally seen. This kind of interaction can simply explain the upshift of the His50 pK_a value from the nominal one (6.8) to 7.7. One would expect that the pK_a of His50 should be shifted down by its location in the hydrophobic core. In fact, the pK_a of His50 is shifted up almost 1 unit, indicating that the interaction of His50 with Glu96 is indeed strong.

The pK_a of Glu96 is not greatly perturbed, since His50 forms a H-bond to its backbone CO, not to that in the side chain. Glu96 has a pK_a of 5.2, which is higher than the intrinsic value, but reasonable considering its local hydrophobic environment.

His137 also has an abnormal pK_a value. The side chain of His137 is clearly buried in the α-sarcin structure, and as expected, its pK_a is lower than that of free histidine. Moreover, the pK_a of histidine 137 is very sensitive to complex formation. This is a common feature of residues strongly involved in enzymatic activity, which allows them to play diverse roles in the different steps of the enzymatic reaction (*16*).

Correlation between pK_a Values and Ribonucleolytic Activity. Extensive studies have been carried out on the α-sarcin enzymatic activity since it was isolated from the mold *A. giganteus* (*56*). Its specific activity against rRNA has been further analyzed (*57*, *58*), but it is not yet well-known how the enzyme interacts with the ribosome and why this interaction is so specific (*52*). In addition to its specific activity against ribosomes, α-sarcin has a residual nonspecific activity against free RNA (*57*), but at higher protein concentrations. Recently, it has been shown that α-sarcin behaves as a cyclizing ribonuclease (*28*) like many other ribonucleases, including RNase T1. First clues about the α-sarcin catalytic mechanism came from sequence comparison, which showed that the protein has a high sequence similarity with RNase T1, a ribonuclease whose enzymatic mechanism has been well studied (*59*). Moreover, superposition of the T1 and α-sarcin structures (*24*) shows that both proteins share identical secondary structure elements and that their catalytic residues occupy the same position and are similarly oriented. All structural and biological evidence indicates that His50, Glu96, and His137 in α-sarcin are the residues involved in catalysis.

The measurements of enzymatic activity against ApA demonstrate that α-sarcin is an acid ribonuclease. Apart from the other ribotoxins of the α-sarcin family (*60*), RNase U2 is the protein phyllogenetically closest to α-sarcin (*61*). Interestingly, the optimum pH for RNase U2 is 4.5 (*62*), which is consistent with the result obtained in this work for α-sarcin (pH 5.0). It can be argued that this optimum pH may be different from the intracellular one. Nevertheless, it has been demonstrated that the possibility of local pH variations related to ribonucleolytic activity of enzymes could result in an optimum pH lower that the physiological pH (*63*). Thus, the presence of different electronic environments in the proximity of the rRNA scissile bond should be taken into account and merits further investigations so the in vivo α-sarcin activity can be better understood.

Table 4: Apparent pK_a Values of Relevant Catalytic Residues[a] in α-Sarcin (this work) and RNase T1[b–d]

	α-sarcin			RNase T1			
	enzymatic activity/pH[e]	NMR			NMR		
residue	vs ApA	wild type	2′-GMP complex	residue	wild type[b]	wild type[c]	wild type[d]
His50	7.8 (7.4−8.0)	7.7 ± 0.2	7.6 ± 0.2	His40	7.9 ± 0.01	7.7 ± 0.2	7.9 ± 0.2
Glu96	3.7 (3.7−3.8)	5.2 ± 0.1	∼4.8	Glu58	4.3 ± 0.05	−	4.1 ± 0.2
His137	6.2 (5.9−6.4)	5.8 ± 0.1	6.8 ± 0.1	His92	7.8 ± 0.01	7.4 ± 0.2	−

[a] Residues H50, E96, and H137 in α-sarcin correspond to H40, E58, and H92 in RNase T1. [b] Reference *68*. [c] Reference *70*. [d] Reference *69*. [e] Values shown are those corresponding to the best fit, and the confidence intervals are given in parentheses.

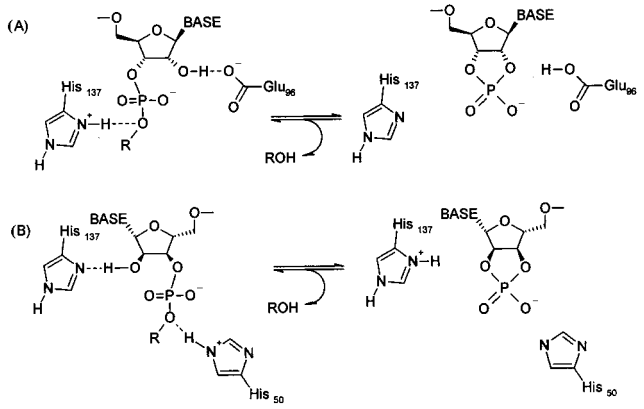

FIGURE 7: Proposed mechanisms for α-sarcin. (A) A general mechanism similar to that of RNase T1, where Glu96 acts as a base and His137 as an acid. (B) A proposed mechanism at basic pH where His50 acts as an acid and His137 as a base.

The mechanism for a nonspecific ribonucleolytic activity is summarized in Figure 7. The transphosphorylation and hydrolysis steps of the reaction follow a concerted in-line mechanism, implying residues acting as a base and an acid located on either side of the scissile bond (*64*). The distinct catalytic roles played by the active site residues in each of these steps depend intimately upon their ionization states, and hence, the activity dependence on pH is determined by pK_a values. In the absence of bound substrate, the apparent pK_a values of His50, Glu96, and His137 are 7.7, 5.2, and 5.8, respectively. In the 2′-GMP complex, the corresponding values are 7.6, ∼4.8, and 6.8, showing that the pK_a values of the active site residues of the α-sarcin are perturbed after substrate binding, mainly that of His137.

The pK_a values calculated for the major peak of α-sarcin activity against the dinucleotide substrate are 3.7 and 6.2. The simplest interpretation of these results is that near pH 5.0, where the enzyme is maximally active, Glu96 exists predominantly in the ionized state and acts as a nucleophile taking a proton from the 2′-OH group in the ribose ring of the nucleotide. Meanwhile, His137 remains protonated to serve as a general acid and acts as a proton donor to the O5′ ester oxygen. Structurally, Glu96 and His137 are on opposite sides of the active center and have the correct geometry for the in-line cleavage of the dinucleotide. His50 is also opposite His137 with respect to the phosphodiester bond so that it could be thought of as an additional candidate for playing the role of a general base. However, the pK_a value of His50 (7.7) ensures that this side chain cannot function as a general base. All these arguments are consistent with a mechanism for α-sarcin similar to that proposed for RNase T1, in which the glutamic acid 58 and the histidine 92 act as a base and acid, respectively. A detailed comparative analysis of the three-dimensional structures of microbial ribonucleases demonstrated that the most common pair of catalytic residues is Glu-His (*65*).

The general mechanism described above is, however, unable to explain the minor peak of activity at neutral pH (Figure 1). Our results for this second mechanism are consistent with a residue playing the role of general base with a pK_a of 6.2, and another one acting as an acid with a pK_a of 7.7. These values are very close to those found in the inhibitor−enzyme complex for His137 (pK_a = 6.8) and for His50 (pK_a = 7.6). In this model, His137 would act at pH 7.0 as a general base and His50 as an acid. This is consistent with the experimental pK_a values, either in the free enzyme or in the complex. At pHs higher than 6.5, His137 and Glu96 populate overwhelmingly the basic form so that they will be unable to act as a general acid in a simple acid−base mechanism. Therefore, the residual enzymatic activity against ApA of α-sarcin near pH 7.0 can be explained in light of this new proposed mechanism with His50 and His137 acting as the catalytic residues. It is probable that the principal difference between the mechanism that predominates at pH 7.0 and the major one that is operating at acidic pH, which is similar to the RNase T1-like mechanism, is a different orientation for parts of the dinucleotide moiety. This interpretation therefore provides an explanation for the two possible catalytic residue pairs, making both mechanisms possible, but the first more efficient.

Ribonucleases are, in general, very versatile enzymes. They act against a great assortment of substrates and under a great variety of microenvironmental conditions (*66*). This implies that their active centers have evolved to accommodate a wide variety of substrates and that the catalytic residues and their mode of action could depend strongly on the substrate. In nature, α-sarcin acts against a single bond in the ribosome. This extreme specificity suggests that its mechanism of action against its natural target may differ in some details from the mechanisms proposed herein based on dinucleotide hydrolysis.

Comparison between α-Sarcin and RNase T1. It is instructive to compare the data found for α-sarcin with those pertaining to the well-characterized RNase T1 (*67*). With respect to the electrostatic behavior, some pK_a values have been reported in the literature for RNase T1 (*68*, *69*, *70*), including those corresponding to the active site residues, His40, Glu58, and His92 (Table 4). The ionization constant reported for His40 in RNase T1 (average pK_a = 7.8) is coincident with that of His50 in α-sarcin. However, pK_a values of Glu58 and His92 in RNase T1 (average pK_a = 4.2 and 7.6, respectively) are significantly different from those

obtained for the equivalent residues Glu96 and His137 in α-sarcin.

There is a general agreement in that His40, Glu58, and His92 in RNase T1 correspond to His50, Glu96, and His137 in α-sarcin. These residues share the same spatial orientation (Figure 6) and are involved in catalysis. However, some other residues such as Tyr38, Arg77, and Phe100 in RNase T1, structurally equivalent to Tyr48, Arg121, and Leu145 in α-sarcin, have also been shown to be important in catalysis (*71*, *72*). In RNase T1, these residues have been postulated to participate in stabilizing the reaction intermediate or the substrate or both (*70*). As can be seen in Figure 6, all these residues are conserved in both structures except Phe100 in RNase T1, which is replaced by Leu145 in α-sarcin. A comparison of the amino acid sequences reveals that the phenylalanine residue at this position is conserved in almost all RNase T1-like microbial ribonucleases but not in α-sarcin-like fungal ribotoxins in which it is substituted by leucine (*60*). In RNase T1, the imidazole ring of His92 is stacked with the aromatic ring of Phe100, whereas in α-sarcin, which lacks Phe, this interaction is not possible. The Phe−His interaction has been studied by ab initio calculations (*51*, *73*) and by CD and NMR spectroscopies (*74*, *75*). These studies show that the π electrons of the phenyl ring of Phe can play the role of a hydrogen bond acceptor (*76*) with the imidazolium group acting as a hydrogen bond donor. The Phe−His interaction is much stronger when the His ring is positively charged (*74*), which is reflected in an increase in the His pK_a value. This interaction itself can explain the higher pK_a value of His92 measured in RNase T1 as compared to that of His137 in α-sarcin.

The different pK_a values of acid histidines (His92 in RNases T1 and His137 in α-sarcin) may explain the differences observed in the enzymatic activity profiles of RNase T1 and α-sarcin. Thus, in RNase T1 the pK_a values of catalytic residues Glu58 and His92 differ by 3.1 units, allowing the protein to be highly active over a wide pH range (broad maximum between pH 3.5 and 7.0) (*70*). In the case of α-sarcin, where the Phe−His interaction is not possible, the pK_a difference falls to only 0.6 unit, reducing both the width and the height of the activity profile to a narrow, low maximum centered around pH 5.0.

Recently, the function of the conserved Phe100 of RNase T1 has been investigated by site-directed mutagenesis (*71*). The reported F100A mutant lacks the Phe−His interaction and shows a k_{cat} reduced 75-fold for the degradation of GpC dinucleotide. In contrast with the hypothesis presented above, the conclusion of this study was that the contribution of Phe100 to catalysis does not involve His92 and may arise from a direct interaction between the aromatic ring of Phe100 and the phosphate moiety of the substrate. Although Doumen and co-workers did not observe a contribution of the Phe−His interaction to catalysis, such a contribution might have been observed if the activity had been measured for a series of different pH values. Our results suggest that the Phe−His interaction does play a role and cannot be neglected. As we have shown, this interaction should affect the His92 pK_a value and consequently the enzymatic activity on the mutant. In summary, the absence of the phenylalanine ring in the catalytic center of α-sarcin or the F100A RNase T1 mutant can account for their reduced enzymatic activity against dinucleotides compared with that of wild-type RNase T1.

Conclusions. This work focused on understanding the contribution of the electrostatic interactions to the α-sarcin stability and activity. With the results presented here, α-sarcin becomes the first fungal ribotoxin fully studied by NMR and joins the small group of proteins whose electrostatic interactions have been extensively characterized. We have determined and assigned the pK_a values of all glutamic acids, histidines, the C-terminal carboxylate, and most of the aspartic acids in the free enzyme to specific residues in the protein. We have also determined the pK_a of the histidine residues in the α-sarcin−2′-GMP complex, and measured for the first time the activity of α-sarcin as a function of pH. The main conclusions of the results presented here are the following. α-Sarcin is an acid ribonuclease with an optimum activity at pH 5.0 and secondary activity at neutral pH that is about 30% of the maximum value. The activity on a dinucleotide substrate can be explained in terms of two different reaction mechanisms. The main mechanism (RNase T1-like) operating at acidic pH involves His137 and Glu96 acting as a general acid and as a general base, respectively. The secondary mechanism operating at pH 7.0 can be explained with His50 and His137 acting as the general acid and base, respectively. In addition, the differences in the enzymatic activity profiles of α-sarcin and RNase T1 can be explained on the basis of the different pK_a values of the catalytic residues measured in this work. In RNase T1, the difference of the catalytic residue pK_a values is large and the protein is active over a wide pH range, between 3.5 and 7.0. In α-sarcin, however, the absence of the Phe−His interaction, which is present in almost all microbial ribonucleases, lowers the pK_a value of the acid histidine (His137) as compared to the corresponding one in RNase T1. Thus, the pK_a difference between the acid and the basic catalytic residues is reduced, which in turn restricts the protein activity to a narrow band centered around pH 5.0.

ACKNOWLEDGMENT

We thank Dr. D. V. Laurents and Dr. J. L. Neira for helpful discussions and suggestions.

REFERENCES

1. Perutz, M. F. (1978) *Science 201*, 1187−1191.
2. Gilson, M. K. (1995) *Curr. Opin. Struct. Biol. 5*, 216−223.
3. Matthew, J. B., Gurd, F. R. N., Garcia-Moreno, B., Flannegan, M. A., March, K. L., and Shire, S. J. (1985) *Crit. Rev. Biochem. 18*, 91−197.
4. Tanford, C. (1962) *Adv. Protein Chem. 17*, 69−165.
5. Yang, A. S., and Honig, B. (1992) *Curr. Opin. Struct. Biol. 2*, 40−45.
6. Pace, C. N., Shirley, B. A., McNutt, M., and Gajiwala, K. (1996) *FASEB J. 10*, 75−83.
7. Hughson, F. M., and Baldwin, R. L. (1989) *Biochemistry 28*, 4415−4422.
8. Nall, B. T., Osterhout, J. J., Jr., and Ramdas, L. (1988) *Biochemistry 27*, 7310−7314.
9. Meadows, D. H., Markley, J. L., Cohen, J. S., and Jardetzky, O. (1967) *Proc. Natl. Acad. Sci. U.S.A. 58*, 1307−1313.
10. Jardetzky, O., Thielmann, H., Arata, Y., Markley, J. L., and Williams, M. N. (1972) *Cold Spring Harbor Symp. Quant. Biol. 36*, 257−261.
11. Markley, J. L. (1973) *Biochemistry 12*, 2245−2250.
12. Kohda, D., Sawada, T., and Inagaki, F. (1991) *Biochemistry 30*, 4896−4900.

13. Forman-Kay, J., Clore, G. M., and Gronenborn, A. M. (1992) *Biochemistry 31*, 3442−3452.
14. Abildgaard, F., Jorgensen, A. M. M., Led, J. J., Christensen, T., Jensen, E. B., Junker, F., and Dalboge, H. (1992) *Biochemistry 31*, 8587−8596.
15. Qin, J., Clore, G. M., and Gronenborn, A. M. (1996) *Biochemistry 35*, 7−13.
16. McIntosh, L. P., Hand, G., Johnson, P. E., Joshi, M. D., Korner, M., Plesniak, L. A., Ziser, L., Wakarchuk, W. W., and Withers, S. G. (1996) *Biochemistry 35*, 9958−9966.
17. Oliveberg, M., Arcus, V. L., and Fersht, A. R. (1995) *Biochemistry 34*, 9424−9433.
18. Tan, Y. J., Oliveberg, M., Davis, B., and Fersht, A. R. (1995) *J. Mol. Biol. 254*, 980−992.
19. Chivers, P. T., Prehoda, K. E., Volkman, B. F., Kim, B. M., Markley, J. L., and Raines, R. T. (1997) *Biochemistry 36*, 14985−14991.
20. Singer, A. U., and Forman-Kay, J. D. (1997) *Protein Sci. 6*, 1910−1919.
21. Wool, I. G. (1984) *Trends Biochem. Sci. 9*, 14−17.
22. Wool, I. G., Glück, A., and Endo, Y. (1992) *Trends Biochem. Sci. 17*, 266−269.
23. Gasset, M., Mancheño, J. M., Lacadena, J., Turnay, J., Olmo, N., Lizarbe, M. A., Martínez del Pozo, A., Oñaderra, M., and Gavilanes, J. G. (1994) *Curr. Top. Pept. Protein Res. 1*, 99−104.
24. Campos-Olivas, R., Bruix, M., Santoro, J., Martínez del Pozo, A., Lacadena, J., Gavilanes, J. G., and Rico, M. (1996) *FEBS Lett. 399*, 163−165.
25. Gasset, M., Oñaderra, M., Thomas, P. G., and Gavilanes, J. G. (1990) *Biochem. J. 265*, 815−822.
26. Gasset, M., Oñaderra, M., Thomas, P. G., and Gavilanes, J. G. (1991) *Biochim. Biophys. Acta 1080*, 51−58.
27. Campos-Olivas, R., Bruix, M., Santoro, J., Martínez del Pozo, A., Lacadena, J., Gavilanes, J. G., and Rico, M. (1996) *Protein Sci. 5*, 969−972.
28. Lacadena, J., Martínez del Pozo, A., Lacadena, V., Martínez-Ruiz, A., Mancheño, J. M., Oñaderra, M., and Gavilanes, J. G. (1998) *FEBS Lett. 424*, 46−48.
29. Lacadena, J., Martínez del Pozo, A., Barbero, J. L., Mancheño, J. M., Gasset, M., Oñaderra, M., Lopez-Otín, C., Ortega, S., García, J., and Gavilanes, J. G. (1994) *Gene 142*, 147−151.
30. Wishart, D. S., Bigam, C. G., Yao, J., Abildgaard, F., Dyson, H. J., Oldfield, E., Markley, J. L., and Sykes, B. D. (1995) *J. Biomol. NMR 6*, 135−140.
31. Marion, D., and Wüthrich, K. (1983) *Biochem. Biophys. Res. Commun. 113*, 967−974.
32. Piotto, M., Saudek, V., and Sklenar, V. (1992) *J. Biomol. NMR 2*, 661−665.
33. Aue, W. P., Bartholdi, E., and Ernst, R. R. (1976) *J. Chem. Phys. 64*, 2229−2246.
34. Bax, A., and Davis, D. G. (1985) *J. Magn. Reson. 65*, 355−360.
35. Kumar, A., Ernst, R. R., and Wüthrich, K. (1980) *Biochem. Biophys. Res. Commun. 95*, 1−6.
36. Wüthrich, K. (1986) *NMR of proteins and nucleic acids*, Wiley, New York.
37. De Marco, A. (1977) *J. Magn. Reson. 26*, 527−528.
38. Bundi, A., and Wüthrich, K. (1979) *Biopolymers 18*, 285−297.
39. Kraulis, P. J. (1989) *J. Magn. Reson. 24*, 627−633.
40. Kraulis, P. J., Domaille, P. J., Campbell-Burk, S. L., van Aken, T., and Laue, E. D. (1994) *Biochemistry 33*, 3515−3531.
41. Sharger, R. I., Cohen, J. S., Heller, S. R., Sachs, D. H., and Schechter, A. N. (1972) *Biochemistry 11*, 541−547.
42. Martínez del Pozo, A., Gasset, M., Oñaderra, M., and Gavilanes, J. G. (1988) *Biochim. Biophys. Acta 953*, 280−288.
43. Petros, A. M., and Fesik, S. W. (1994) *Methods Enzymol. 176*, 717−739.
44. Toiron, C., González, C., Bruix, M., and Rico, M. (1996) *Protein Sci. 5*, 1633−1647.
45. Shimada, I., and Inagaki, F. (1990) *Biochemistry 29*, 757−764.
46. Yang, X., and Moffat, K. (1996) *Structure 4*, 837−852.
47. States, D. J., and Karplus, M. (1987*) J. Mol. Biol. 197*, 122−130.
48. Tanford, C., and Kirkwood, J. G. (1957) *J. Am. Chem. Soc. 79*, 5333−5339.
49. Campos-Olivas, R. (1997) Ph.D. Thesis, Universidad Complutense de Madrid, Madrid, Spain.
50. Bermejo, F. J., Rico, M., Santoro, J., Herranz, J., Gallego, E., and Nieto, J. L. (1986) *J. Mol. Struct. 142*, 339−342.
51. Fernández-Recio, J., Vázquez, A., Civera, C., Sevilla, P., and Sancho, J. (1997) *J. Mol. Biol. 267*, 184−197.
52. Kao, R., and Davies, J. (1995) *Biochem. Cell Biol. 73*, 1151−1159.
53. Glück, A., and Wool, I. G. (1996) *J. Mol. Biol. 256*, 838−848.
54. Bourne, H. R., Sanders, D. A., and McCormick, F. (1991) *Nature 349*, 117−127.
55. Honig, B. H., and Hubbell, W. L. (1984) *Proc. Natl. Acad. Sci. U.S.A. 81*, 5412−5416.
56. Olson, B. H., and Goerner, G. L. (1965) *Appl. Microbiol. 13*, 314−321.
57. Endo, Y., and Wool, I. G. (1982) *J. Biol. Chem. 257*, 9054−9060.
58. Endo, Y., Huber, P. W., and Wool, I. G. (1983) *J. Biol. Chem. 258*, 2662−2667.
59. Steyaert, J. (1997) *Eur. J. Biochem. 247*, 1−11.
60. Wirth, J., Martínez del Pozo, A., Mancheño, J. M., Martínez-Ruiz, A., Lacadena, J., Oñaderra, M., and Gavilanes, J. G. (1997) *Arch. Biochem. Biophys. 343*, 188−193.
61. Mancheño, J. M., Gasset, M., Lacadena, J., Martínez del Pozo, A., Oñaderra, M., and Gavilanes, J. G. (1995) *J. Theor. Biol. 172*, 259−267.
62. Arima, T., Uchida, T., and Egami, F. (1968) *Biochem. J. 106*, 601−607.
63. García-Segura, J. M., Fominaya, J. M., Orozco, M. M., and Gavilanes, J. G. (1986) *Eur. J. Biochem. 18*, 229−233.
64. Saenger, W. (1991) *Curr. Opin. Struct. Biol. 1*, 130−138.
65. Nonaka, T., Nakamura, K. T., Uesugi, S., Ikehara, M., Irie, M., and Mitsui, Y. (1993) *Biochemistry 32*, 11825−11837.
66. Wool, I. G. (1997) *Ribonucleases, structure and functions*, pp 131−162, Academic Press, New York.
67. Irie, M. (1997) *Ribonucleases, structure and functions*, pp 101−130, Academic Press, New York.
68. Inagaki, F., Kawano, Y., Shimida, I., Takahashi, K., and Miyazawa, T. (1981) *J. Biochem. (Tokyo) 89*, 1185−1195.
69. McNutt, M., Mullins, L. S., Raushel, F. M., and Pace, C. M. (1990) *Biochemistry 29*, 7572−7576.
70. Steyaert, J., Hallenga, K., Wyns, L., and Stanssens, P. (1990) *Eur. J. Biochem. 29*, 9064−9072.
71. Doumen, J., Gonciarz, M., Zegers, I., Loris, R., Wyns, L., and Steyaert, J. (1996) *Protein Sci. 8*, 1523−1530.
72. Grunert, H. P., Zouni, A., Beineke, M., Quaas, R., Georgalis, Y., Saenger, W., and Hahn, U. (1991) *Eur. J. Biochem. 197*, 203−207.
73. Fowler, P. W., and Moore, G. J. (1988) *Biochem. Biophys. Res. Commun. 153*, 1296−1300.
74. Shoemaker, K. R., Fairman, R., Schultz, D. A., Robertson, A. D., York, E. J., Stewart, J. M., and Baldwin, R. L. (1990*) Biopolymers 29*, 1−11.
75. Armstrong, K. M., Fairman, R., and Baldwin, R. L. (1993) *J. Mol. Biol. 230*, 284−291.
76. Levitt, M., and Perutz, M. F. (1988) *J. Mol. Biol. 201*, 751−754.
77. Kraulis, P. J. (1991) *J. Appl. Crystallogr. 24*, 946−950.
78. Pfeiffer, S., Karini-Nejad, Y., and Rüterjans, H. (1997) *J. Mol. Biol. 266*, 400−423.

BI981672T